Microwave Engineering
Ulm University

ulm university universität
uulm

Increasing the Efficiency and Robustness of Angular Radar Calibration by Exploiting Phase Symmetry

André Dürr, Matthias Linder, and Christian Waldschmidt

© 2020 IEEE. Personal use of this material is permitted. Permission from IEEE must be obtained for all other uses, in any current or future media, including reprinting/republishing this material for advertising or promotional purposes, creating new collective works, for resale or redistribution to servers or lists, or reuse of any copyrighted component of this work in other works.
DOI: 10.1109/EuRAD48048.2021.00019

Increasing the Efficiency and Robustness of Angular Radar Calibration by Exploiting Phase Symmetry

André Dürr[1], Matthias Linder, and Christian Waldschmidt
Institute of Microwave Engineering, Ulm University, 89081 Ulm, Germany
[1]andre.duerr@uni-ulm.de

***Abstract* — For imaging radars, the calibration effort increases with higher frequency and finer angular resolution demands and is therefore one of the largest cost factors in radar production. In case of high angular resolution, the calibration is also sensitive to array misalignment, resulting in costly calibration procedures. This paper proposes an angle-dependent radar calibration method with significantly reduced calibration effort. The high efficiency and robustness against misalignment is achieved by exploiting phase symmetry of a target in the measured radar response. Based on an initial theoretical formulation followed by an experimental verification, this novel approach does not only yield a cost-effective calibration, but also increases the robustness against array misalignment.**

***Keywords* — Calibration, direction-of-arrival estimation, imaging radar, millimeter wave radar, phase center.**

I. Introduction

Future radar applications require radar sensors with an improved detection performance in range, velocity, and angle [1]. Typically, a time-consuming angle-dependent calibration with an angular step size below the resolution of the array is required to determine the calibration parameters required for direction-of-arrival (DoA) estimation [2], [3], [4]. Consequently, the calibration is one of the largest cost factors in radar production [5].

For most radar applications, the estimation of the DoA is based on digital beamforming on the receiver side. The required steering vector for DoA estimation is extracted from the corresponding range-velocity bin of the detected target in each channel [6], [7], [8]. Especially at frequencies in the upper millimeter wave range (above 100 GHz), the performance in DoA estimation is sensitive to antenna misalignment due to the small wavelength and mutual antenna coupling, which are the main contributions for a deviation between ideal array model and the electrical behavior of the antennas. This increasing deviation between the desired antenna positions and the electrical behavior of the antennas requires to calibrate the antenna locations (phase centers) in order to obtain an accurate DoA estimation [5], [9].

In this paper, an angle-dependent radar calibration with high accuracy of the determined calibration parameters is proposed. It will be shown that the number of measuring points can be reduced significantly compared to common calibration methods. The phase center and the individual phase offset for each receive (RX) antenna are determined by exploiting symmetry in the phase pattern. The reliability and accuracy of the method is proven by measurements.

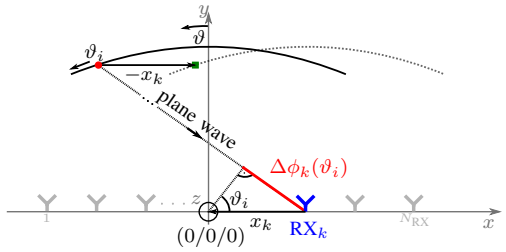

Fig. 1. Calibration set-up and reference coordinate system for a an antenna array and an exemplary highlighted receive antenna (Y) located outside the measurement origin. The calibration target is moving on a trajectory around the measurement origin in the far-field ($r \gg x_k$) of the array (●). The steering vector at the angle ϑ_i is modified as if the virtual target (■) is measured.

II. DoA Estimation with DFT

Depending on the incident angle of the wave at the k-th RX antenna of an antenna array, an additional phase shift w. r. t. the adjacent antenna occurs. In general, the angular spectrum $\mathbf{P}(\vartheta)$ is obtained by a discrete Fourier transform (DFT), where the n-th entry P_n is given by [5]

$$P_n = \sum_{k=1}^{N_{\mathrm{RX}}} s_k \mathrm{e}^{-\mathrm{j}\phi_k} \mathrm{e}^{-\mathrm{j}2\pi \frac{k'}{N_{\mathrm{ZP}}} n}\,, \tag{1}$$

$$\text{with} \quad k' = \frac{x_k}{\lambda_0/2}\,, \quad N_{\mathrm{ZP}} = \frac{180^\circ}{\delta\vartheta}\,,$$

$$n \in \left[\sin(\vartheta_{\max})\frac{-90^\circ}{\delta\vartheta}, \sin(\vartheta_{\max})\frac{90^\circ}{\delta\vartheta}\right] \cap \mathbb{Z}\,. \tag{2}$$

In (1), $\mathbf{s} = (s_1, \ldots, s_{N_{\mathrm{RX}}})$ denotes the steering vector, ϕ_k is the individual phase offset at the k-th RX antenna at boresight due to hardware imperfections, k' is the fractional value of the antenna location x_k, λ_0 is the free-space wavelength, N_{ZP} is the overall number of Fourier samples according to the desired angular grid resolution $\delta\vartheta$, and $\pm\sin(\vartheta_{\max})$ is the angular field of view. At millimeter wave frequencies, a deviation between the physical antenna position and the electrical behavior of the antenna occurs due to mutual antenna coupling or manufacturing uncertainties [5]. Apart from the individual phase offset ϕ_k determined in common radar calibration, the true electrical antenna position x_k is therefore unknown and must be determined by calibration.

III. Calibration Concepts

The calibration set-up and reference coordinate system are given in Fig. 1 for an exemplary RX antenna (Y) on the x-axis

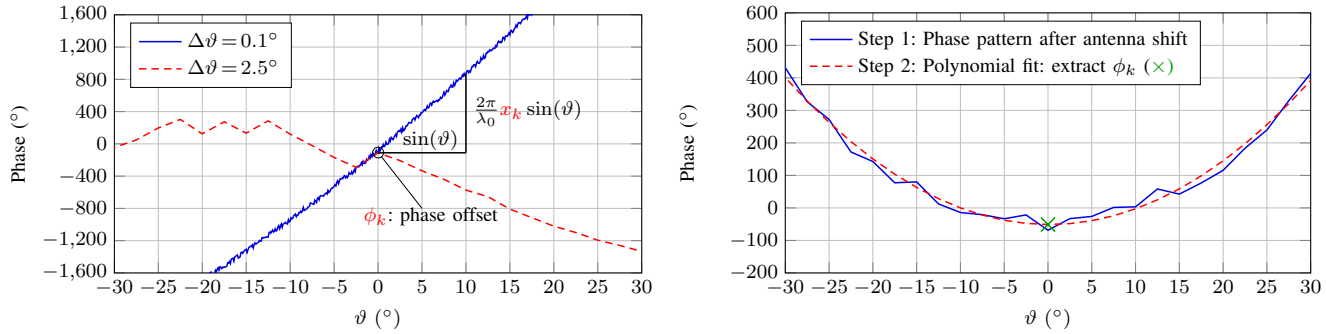

(a) (b)

Fig. 2. Measured phase pattern at an exemplary RX antenna. (a) Calibration based on the phase progression for different angular step sizes. (b) Calibration based on the phase symmetry with an angular step size $\Delta\vartheta = 2.5°$.

and a calibration target (●) in the far-field at distance r from the antenna. The phase center of an antenna is defined as the origin of a spherical wave emitted by the antenna. Without loss of generality, the phase center of the k-th antenna is located at the unknown distance x_k from the measurement origin.

A. Calibration Based on Phase Progression

According to the calibration set-up in Fig. 1, the angle-dependent phase progression $\Delta\phi_k$ of a plane wave impinging on the k-th RX antenna is given by

$$\Delta\phi_k(\vartheta) = \frac{2\pi}{\lambda_0} x_k \sin(\vartheta) + \phi_k \,. \tag{3}$$

This phase trend is evaluated in Fig. 2 (a) for two different angular step sizes $\Delta\vartheta$. In case of large arrays, the change in phase for two successive angular steps at distant antennas from the array center might exceed 180°, leading to phase ambiguities. However, a sufficiently small angular step size eliminates ambiguities and allows to determine the phase center x_k and the phase offset ϕ_k required for the DoA estimation in Section II by means of linear regression, see Fig. 2 (a). For a reliable parameter extraction based on data without phase ambiguities, the angular step size $\Delta\vartheta$ must fulfill

$$\Delta\phi_{\max} = 360° \frac{x}{\lambda_0} \sin(\Delta\vartheta)\Big|_{x=\begin{cases}|\max\{x_k\}|\\|\min\{x_k\}|\end{cases}} \ll 180° \,. \tag{4}$$

Consequently, the angular step size must be reduced for increasingly large aperture sizes $A_V = |\max\{x_k\} - \min\{x_k\}|$.

B. Calibration Based on Phase Symmetry

In contrast to the calibration method based on phase progression, phase ambiguities (see Fig. 2 (a), - - -) can be significantly reduced if symmetry in the phase pattern is exploited. As shown for antenna measurements [10], asymmetries in the phase pattern of the measured RX signal can be used to determine the phase center of an antenna. Since the bandwidth of radars is relatively small compared to the center frequency, the signal can be considered as narrowband. This allows to adopt this method for radar calibration.

The calibration method based on phase symmetry can be subdivided into the following two steps:

1) Determine the Phase Center of the Antenna

In the following, a calibration target moves on a trajectory with radius r around the origin of the measurement coordinate system (see Fig. 1). The measured distance of the target at the k-th RX antenna and the corresponding phase of the target in the radar response differs for each measurement angle ϑ_i as the antenna is located outside the measurement origin. To determine the unknown phase center x_k of the k-th RX antenna, the position of the antenna is virtually shifted along the x-axis to achieve maximum phase symmetry. By means of a global search with all possible antenna position shifts (grid resolution: $\lambda_0/20$), the optimum shift is evaluated in each measurement plane. Therefore, the symmetry metric

$$S = \sum_{i=1}^{\lfloor M/2 \rfloor} |\phi_{M+1-i} - \phi_i| \tag{5}$$

shall be minimized. In (5), ϕ_i denotes the phase of the target in the radar response at the angle $\vartheta_i \in [-\vartheta_{\max}, \vartheta_{\max}]$ and $i \in [1, \ldots, M]$ the measurement number. A low value S corresponds to a high phase symmetry [cf. Fig. 2 (b)].

The measured entries of the steering vector s_{k_i} for each measurement i at the angle ϑ_i are modified with the same virtual antenna shift along the x-axis (see Fig. 2 (b), ——). A path difference x_k between the k-th RX antenna and the measurement origin corresponds to a change in phase of $\Delta\tilde{\phi}_k(\vartheta_i) = 2\pi x_k \sin(\vartheta_i)/\lambda_0$ [cf. (3)]. Thus, the measured entry of the steering vector is modified by

$$s'_{k_i} = s_{k_i} \exp\left(-\mathrm{j}\Delta\tilde{\phi}_k(\vartheta_i)\right) = |s_{k_i}|\, \mathrm{e}^{\mathrm{j}\phi_{k_i}} \,, \tag{6}$$

which coincides with a measurement of the virtual target (●) or, alternatively, with a shift of the phase center of the antenna to the origin of the measurement coordinate system. Without loss of generality, this procedure can be extended to a 2-D lattice of antennas. However, to remain ambiguous-free, the measurement has to be performed in two orthogonal planes.

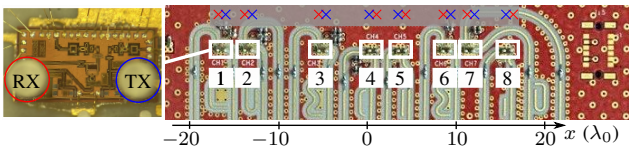

Fig. 3. Photograph of the antenna array consisting of eight MMICs, each incorporating one transmit (TX, ×) and one RX (×) antenna.

Table 1. Overview of the radar parameters

Ramp duration T	100 µs
Center frequency f_c	152.5 GHz
RF bandwidth B	10 GHz
Number of chirps N_c	512
Number of virtual channels N_{VX}	$64 = 8 \times 8$
Virtual aperture size A_V	$65\,\lambda_0$

2) *Polynomial Fit of the Modified Phase Pattern*

Due to a small displacement in y-direction, r changes symmetrically for positive and negative angles. Thus, the modified phase pattern results in a parabola and not in a straight line. Based on a polynomial fit of 2nd order, the phase offset ϕ_k is extracted from regression at the angle $\vartheta_i = 0°$.

In case of a spherical incident wave (far-field condition not valid), the k-th RX antenna experiences a phase progression for a target located at $\vartheta_i = 0°$. Thus, the phase offset ϕ_k has to be corrected by means of an optical path model.

IV. Measurement Verification

The performance of the symmetry-based calibration is proven by measurements regarding the accuracy of the determined calibration parameters, the performance in angular estimation, and robustness against misalignment. Afterwards, it is compared to the calibration based on phase progression.

A. *Radar Demonstrator*

A photograph of the 160 GHz frequency-modulated continuous-wave (FMCW) radar front end consisting of 8 monolithic microwave integrated circuits (MMICs), each incorporating one TX and one RX antenna, is shown in Fig. 3. The radar is operated with the radar parameters summarized in Table 1. For further information on the radar demonstrator and the antenna array, see [9].

B. *Accuracy of the determined Calibration Parameters*

To demonstrate the efficiency of both calibration methods in comparison, the radar is calibrated with an angular step size $\Delta\vartheta = 0.1°$ according to Fig. 1. Afterwards, the phase centers x_k and phase offsets ϕ_k are evaluated in terms of the angular step size $\Delta\vartheta$ by omitting measuring points. As shown in Fig. 4, both calibration methods provide identical phase centers x_k and phase offsets ϕ_k for small angular step sizes [$< 0.8°$, theoretical limit: $0.88°$, cf. (4)]. For larger angular step sizes $\Delta\vartheta$, the phase progression approach results in phase ambiguities leading to a regression line with reduced slope [cf. Fig. 2 (a)]. Thus, the estimated antenna positions and

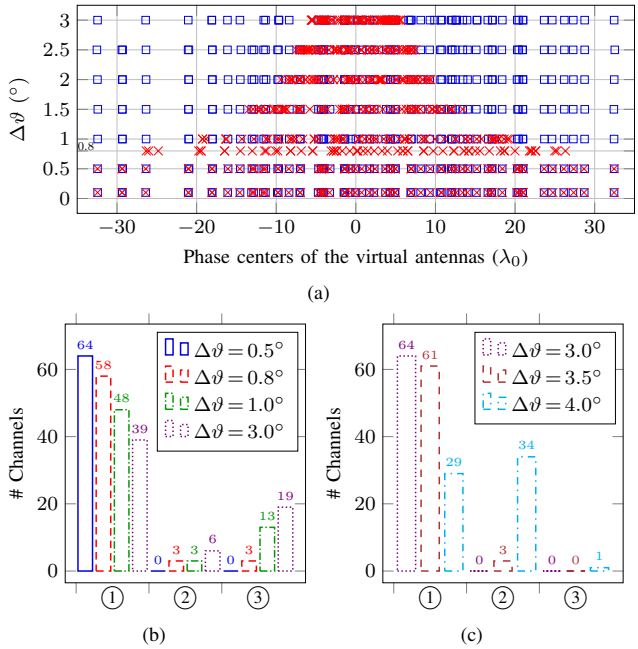

Fig. 4. Accuracy of determined calibration parameters. (a) Phase centers of virtual antennas obtained from the calibration using phase symmetry (□) and using phase progression (×). Phase error of the phase offset ε_{ϕ_k} for (b) the phase progression method and (c) for the phase symmetry method. ① $\varepsilon_{\phi_k} < 20°$, ② $20° < \varepsilon_{\phi_k} \leq 80°$, ③ $\varepsilon_{\phi_k} > 80°$.

the resulting virtual array become smaller [see Fig. 4 (a)]. In contrast, using the symmetry approach, the angular step size can be increased up to 3° without any significant deviation from the phase centers obtained by a step size of 0.1°. The phase error of the phase offset ε_{ϕ_k} is defined as the deviation from the standard calibration with a step size of 0.1°. As shown in Fig. 4 (b) and (c), when using phase symmetry, the phase error of the phase offset is much less error-prone. The phase offset can be determined very accurately up to a step size of $\Delta\vartheta = 3.5°$ whereas an angular step size below 0.8° is necessary for the method based on phase progression.

C. *Performance in Angular Estimation*

The performance in DoA estimation is now evaluated using both calibration techniques for a target, which is located at the distance $R = 3.6$ m and the angle $\vartheta = -20°$. The measurement results are depicted in Fig. 5. The same measurement data is employed with a different angular step size $\Delta\vartheta$ used for the calibration. Starting from an angular step size of 0.8°, the phase progression method results in increasing deviations w. r. t. the calibration with a step size of 0.1° [Fig. 5 (a)]. Additionally, the target peak is broadened due to the decreasing aperture size as shown in Fig. 4 (a). For the symmetry-based calibration method, there is no noticeable change in the angular spectrum up to an angular step size of 2.5° in the calibration. This is also illustrated by the absolute mean error and the corresponding standard deviation given in Tab. 2 for a different number of measuring points in comparison to the reference

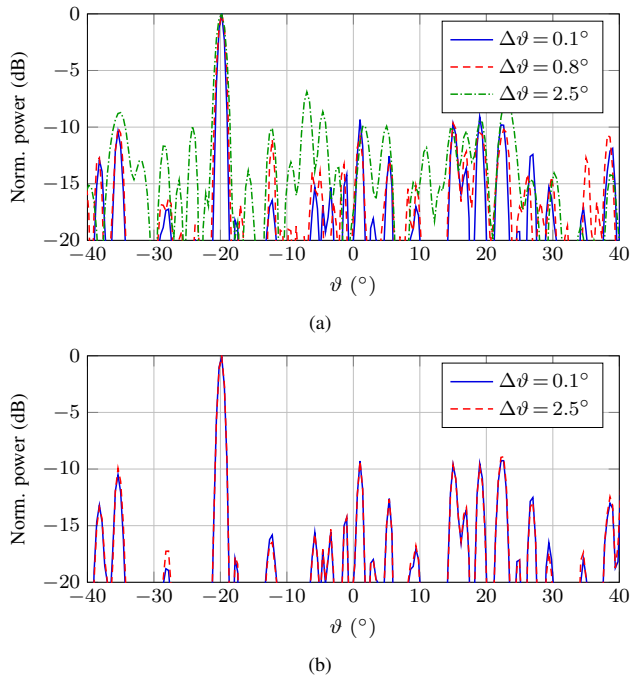

(a)

(b)

Fig. 5. DoA estimation results for a target located at the incident angle $\vartheta = -20°$ in dependency of different calibration step sizes $\Delta\vartheta$. (a) Calibration based on phase progression. (b) Calibration based on phase symmetry.

Table 2. Mean error (ME) and standard deviation (SD) of the angular spectrum in Fig. 5 for both calibration approaches in comparison.

$\Delta\vartheta$	Cal. phase progression (ME/SD)	Cal. symmetry (ME/SD)
0.8°	−19 dB/−16.9 dB	−32.9 dB/−31.2 dB
1.0°	−15.8 dB/−13.2 dB	−31.5 dB/−29.8 dB
2.5°	−12.61 dB/−9.1 dB	−29.6 dB/−24.92 dB

calibration with a step size of 0.1°. The small mean error and standard deviation prove that only negligible deviations occur up to an angular step size of 2.5° in case of the symmetry-based calibration. In contrast, the method based on phase progression is influenced by clearly larger deviations already starting from an angular step size of 0.8°.

D. Robustness against Misalignment

A misalignment of the whole array in x-direction leads to an increased antenna distance from the array center. According to (3), the phase progression is increased and phase ambiguities occur for smaller angular step sizes. Fig. 6 shows the resulting phase centers of the antennas for a misalignment of $\Delta x = 15\,\lambda_0\,(\hat{=}\,3\,\mathrm{cm})$ in dependency of varying angular step sizes. For the calibration based on phase progression, deviations from the correct phase centers of the antennas occur for an angular step size above 0.3° instead of above 0.7° [cf. Fig. 4 (a)]. In contrast, using phase symmetry, there is no noticeable change in the phase centers of the antennas up to an angular step size of 2.5°. Thus, the calibration data is also insensitive to array misalignment.

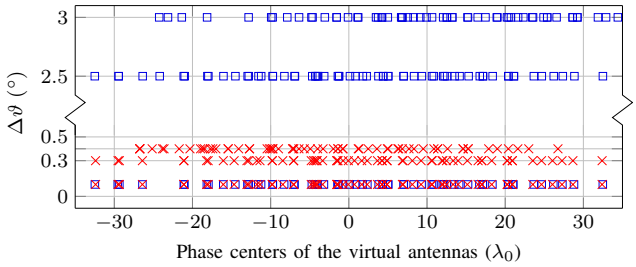

Fig. 6. Robustness against misalignment using the calibration method based on the phase-symmetry (□) and based on the phase progression (×) for a misalignment in x-direction of $\Delta x = 15\,\lambda_0\,(\hat{=}\,3\,\mathrm{cm})$.

V. Conclusion

A novel angle-dependent calibration technique exploiting the phase symmetry of the measured radar response has been proposed and compared to a common calibration method using the angle-dependent phase progression of antennas. Based on measurement results, it is shown that a significant reduction of calibration samples up to a factor of 4 is achieved while preserving the estimation performance. Moreover, an enhanced robustness against array misalignment is achieved, thus allowing a reliable and cost-effective calibration of future radar systems with high angular resolution.

Acknowledgment

This work is funded by the German Research Foundation under project number 317632307.

References

[1] C. Waldschmidt and H. Meinel, "Future Trends and Directions in Radar Concerning the Application for Autonomous Driving," in *European Radar Conference*, Oct. 2014, pp. 416–419.

[2] D. Zankl *et al.*, "BLASTDAR—A Large Radar Sensor Array System for Blast Furnace Burden Surface Imaging," *IEEE Sensors Journal*, vol. 15, no. 10, pp. 5893–5909, Oct. 2015.

[3] P. Heidenreich, "Antenna Array Processing: Autocalibration and Fast High-Resolution Methods for Automotive Radar," Ph.D. dissertation, Technical University of Darmstadt, 2012.

[4] G. Körner *et al.*, "Calibration of MIMO Fully Polarimetric Imaging Radar Systems with Passive Targets," *Frequenz*, 2019.

[5] A. Dürr *et al.*, "On the Calibration of mm-Wave MIMO Radars Using Sparse Antenna Arrays for DoA Estimation," in *European Radar Conference*, Oct. 2019.

[6] P. Stoica and K. C. Sharman, "Maximum Likelihood Methods for Direction-of-Arrival Estimation," *IEEE Trans. Acoust., Speech, Signal Process.*, vol. 38, no. 7, pp. 1132–1143, 1990.

[7] C. Fischer *et al.*, "Evaluation of Different Super-Resolution Techniques for Automotive Applications," in *IET International Conference on Radar Systems*, Oct. 2012, pp. 1–6.

[8] T. S. Dhope, "Application of MUSIC, ESPRIT and ROOT MUSIC in DOA Estimation," *Faculty of Electrical Engineering and Computing, University of Zagreb, Croatia*, 2010.

[9] A. Dürr *et al.*, "High-Resolution 160-GHz Imaging MIMO Radar Using MMICs With On-Chip Frequency Synthesizers," *IEEE Trans. Microw. Theory Techn.*, vol. 67, no. 9, pp. 3897–3907, Sep. 2019.

[10] L. Boehm *et al.*, "Enhancements in mm-wave antenna measurements: automatic alignment and achievable accuracy," *IET Microwaves, Antennas Propagation*, vol. 11, no. 12, pp. 1676–1680, 2017.